RSC Advances

The Impact Of Different ZnO Growth Methods on the Electrical and Optical Properties of a n-ZnO/p-GaN:Mg/c-Plane Sapphire UV LED

Journal:	*RSC Advances*
Manuscript ID:	RA-ART-01-2014-000222.R1
Article Type:	Paper
Date Submitted by the Author:	16-Feb-2014
Complete List of Authors:	FİAT VAROL, Songul; Energy systems engineering, Sahin, Derya; Faculty of Arts And Sciences, Physics Kompitsas, M.; Theor. & Phys./Chem. Institute, Cankaya, Guven; Materials Science and Nanotechnology,

The Impact Of Different ZnO Growth Methods on the Electrical and Optical Properties of a n-ZnO/p-GaN:Mg/c-Plane Sapphire UV LED

Songül FİAT VAROL[1], Derya ŞAHİN[2], Michael KOMPİTSAS[3], Güven ÇANKAYA[4]

[1]Dumlupinar University, Technology Faculty, Energy Systems Engineering, 43500 Kütahya, TÜRKİYE
[2]Gaziosmanpaşa University, Faculty of Arts and Sciences, Physics Department, 60240 Tokat, TURKİYE
[3]National Hellenic Research Foundation, Theoretical and Physical Chemistry Institute, 11635 Athens, GREECE
[4]Yıldırım Beyazıt University, Faculty of Engineering and Natural Sciences, Materials Engineering,06030 Ankara, TÜRKİYE

Abstract

ZnO films were successfully grown on GaN/sapphire by Pulsed Laser Deposition (PLD) and Sol-gel technique. The purpose was to study the effect of each method on the properties of n-ZnO/p-GaN/sapphire UV LED device. The PLD grown ZnO films were obtained at 20 Pa and 30 Pa ambient oxygen pressure while the sol gel grown ZnO films were evaluated as annealed films and as deposited films. It was found that the device performance is strongly depending on ZnO layer deposition method. The present work demonstrates the ability of both chemical and physical growth methods (sol gel and PLD, respectively) to develop high quality ZnO nanofilms with tailored optical properties by selecting the growth conditions. The obtained results show the importance for further studies on the heterojunction ZnO/GaN as a UV LED promising a wide range of applications.

Keywords: ZnO; GaN; Sol-Gel; Pulsed Laser Deposition; LED.

* Corresponding author: Songül FİAT VAROL
Fax: +90 274 513 79 14
Tel: +90 274 265 20 31
E-mail address: songulfiat@yahoo.com

1. Introduction

Wide-band-gap semiconductors GaN and ZnO attract much attention for application in optoelectronic devices such as blue light-emitting diodes (LED), laser diode (LD), and ultraviolet photodetector (PD) [1–3]. They both perfectly share the same crystal structure (wurtzite) and the same stacking sequence (2H) [4], and their lattice mismatches are 1.9% and 0.4% along the a axis and c axis, respectively. Among these, ZnO (Eg = 3.37 eV) is considered a more promising material for next generation UV LEDs [4, 5] and LDs because it has a much larger exciton binding energy than GaN (~60 meV, as opposed to 21 meV), which could lead to UV sources with higher brightness, lower threshold current, better performance at high temperature, and very high radiation resistance [6].

The ZnO-based LEDs will be brighter than the current state-of-art nitride light emitters, and at the same time, the production cost will be reduced significantly compared with current technology. ZnO has some fundamental advantages over its major rival (GaN) as a room temperature emitter, including a more stable exciton, the availability of large-area substrates, the amenability to wet chemical etching, and relatively low materials costs [7, 8]. To match the ZnO based LEDs performance, GaN is a perfect candidate because it has similar crystal structure; furthermore, the thermal expansion coefficients of ZnO are close to those of GaN. Recently, ZnO films have been grown on GaN template using molecular beam epitaxy, metal-organic chemical vapor deposition, magnetron sputtering, pulsed laser deposition (PLD), sol-gel etc. [9-15]. In addition, the exploration of new preparation methods is still in progress.

Stamataki et al. [16] produced transparent ZnO thin films with PLD and reported the annealing effect on structural, electrical and H_2 sensing properties. On the other hand, Tsoutsouva et al. [17] examined the structural, optical, and electrical properties of the as-prepared Zinc oxide (ZnO) thin films deposited on soda lime glass substrates by pulsed laser deposition (PLD) in an oxygen-reactive atmosphere. They studied the dependence of substrate temperature and oxygen pressure.

In ref. [18], researchers saw the high-quality heteroepitaxial ZnO films on GaN-buffered Al_2O_3 substrate by low-temperature hydrothermal synthesis. The room-temperature PL of ZnO film reveals only a main peak at 380 nm without any defect-related deep-level emission. Rogers et al. [19] were reported on the p–n heterojunction LED from ZnO/GaN/Al_2O_3 using pulsed laser deposition method. Both room temperature PL and EL showed an intense main peak at 375 nm with negligibly low green emission. One of these similar works has been accomplished by Yang et al. and Young Lee et al. [20, 21]. They fabricated heterojunction LEDs with an n-

ZnO/p-GaN structure on a c-Al_2O_3 substrate. On the other side, Hwang et al. [22] reported on the growth and device properties of p-ZnO/n-GaN heterojunction LEDs. They examined the I–V characteristics of the Ti/Al and NiO/Au metal contacts on n-type GaN and p-type ZnO films, respectively, and it was found that good ohmic contacts were formed on both electrodes. The PL spectra showed emission peaks of n-type GaN and p-type ZnO at 365 and 385 nm, respectively. In addition to these valuable contributions, Mandalapu et al. [23] added a work of heterojunction LED by growing Sb-doped p-type ZnO layer on an n-type Si substrate. A thin undoped ZnO film was grown at low temperature on n-type Si (100) substrate as a buffer layer, followed by Sb doped ZnO layer at a higher temperature by MBE. Also Park and Yi [24] reported on a p-n heterojunction LED composed of n-type ZnO nanorod on Mg doped p-type GaN film grown by using MOCVD. The main emission peak of EL spectra was a wide yellow emission band centered at 2.2 eV, and the intensity showed an increase with the reverse bias increased from 3 to 7 V. The blue emission peak at 2.8 eV and UV emission peak at 3.35 eV were revealed above reverse-bias voltage of 4 V. For different substrate attempts; Sun et al. [25] tried to make a p-n heterojunction LED composed of n-type ZnO nanorods and p-type Si. The I–V characteristics of n-ZnO nanorods/p-Si heterojunction showed a low threshold voltage under reverse bias and a high resistance under forward bias because of an inconsistent band structure at the interface and the nonideal contact. Then Ling et al. [26] tried $CuAlO_2$ to form n-ZnO nanorod/p-$CuAlO_2$ film heterojunction LED on p-type Si substrates. The LED with the p-type $CuAlO_2$ film indicated a comparatively low turn-on voltage of 4 V and a high breakdown voltage above 40 V compared to the LED without p-type $CuAlO_2$. Also polymer based substrates can be seen in literature with ZnO like Nadarajah's group work [27]. After scanning all these works, we reached to this conclusion that to propound a high quality device; growth technique, selected materials and their consistency as structural, optical etc. have vital importance but also conditions have the same value. We have seen both sol-gel and PLD effect at the same period and on same GaN layers with the same conditions. So, the evaluation and comparison of the techniques for the device performance were more persuasive for us. To date, however, there have been few publications reporting a comparison between the techniques to obtain an enhanced device and even fewer with all details of the electrical and morphological properties. Also oxygen pressure effect has not been considered yet on n-ZnO/p-GaN LED characterization.

2. Experimental details

A ~700 nm thick Mg doped GaN layer (GaN:Mg) was grown on a c-sapphire (0 0 0 1) substrate (2 cm∗2 cm) by Metal–Organic Chemical Vapor Deposition (MOCVD) by using a low-pressure horizontal-flow reactor. Trimethylgallium (C_3H_9Ga), ammonia (NH_3) and bis(cyclopentadienyl) magnesium (CP_2Mg) were used as the precursors for Ga, N and Mg, respectively [28, 29]. Prior to the film growth, (0 0 0 1) sapphire substrates have been sequentially cleaned with methanol, acetone and distilled water in the ultrasonic cleaner. For the film growth, the substrate temperature was maintained at 500 °C and the deposition time was 30 min. Heat treatment at 650 °C for 10 min in ambient nitrogen activated the p-type dopant.

The thickness of GaN thin films was measured at about 50 nm. Hall Effect measurements of the p-type GaN layer revealed a hole concentration of ~8.0 x10^{17} cm^{-3} and mobility of 4.2 cm^2 V^{-1} s^{-1}. The resistivity of the film was also measured at 1.2 ohm-cm.

Subsequently, ZnO thin films, grown either by sol gel or Pulsed Laser Deposition (PLD) have been deposited onto the GaN/ sapphire substrates.

2.1 Sol-Gel Process

Before growth in the aqueous solution, the GaN substrate was cleaned in deionized water, ethanol, and acetone. In a typical sol gel technique, zinc acetate dihydrate $Zn(CH_3COO)_2.2H_2O$ were first dissolved in a mixture of 2-methoxyethanol and monoethanolamine (MEA) at room temperature [30]. The concentration of zinc acetate was 0.7mol/l. The molar ratio of monoethanolamine to zinc acetate was kept at 1:1. The pH value has changed from 6.0 to 10.5 with MEA. The alkaline nature of the sol has been reported to help the growth of ZnO.

The precursor solution was mixed with a magnetic stirrer at 60 °C for 2 h to get a clear and homogeneous sol. Diethanolamine (DEA) was added to increase the solubility, then stirred with the magnetic stirrer at 50-60°C for 1 h again. Finally, the solution was stirred by a magnetic stirrer at 70–80 °C for 2 h to get a clear, homogeneous and transparent sol, which served as the coating sol after standing for 2 days. Then, the sol was dropped on the p-type GaN substrates, which was spun at 2000 rpm for 1min (Fig.1a). After spin coating, the substrates were kept at 300 °C for 10 min in a tube furnace, for the solvent to evaporate and

eliminate the organic component in the thin films. The aforementioned procedure was repeated 5 times to deposit films with the desired thickness.

Two grown undoped n-type ZnO layers had ~$1.1x10^{16}$ cm^{-3} and ~$4x10^{16}$ cm^{-3} carrier concentrations that followed from Hall Effect measurement. Their thickness values were ~ 700 nm and 650 nm, respectively.

2.2 Pulsed Laser Deposition (PLD) Process

ZnO films were deposited on GaN substrates by using an UV pulsed KrF excimer laser operated at 248nm, with 10 Hz pulse repetition rate pulse duration 10 ns. A laser fluence of 1.5 J/cm^2 was used to ablate the metallic Zn target which consisted of a Zn disk (Aldrich 99.9% purity), with diameter 1.5 cm and thickness 0.5 cm, and was placed at a distance of 5 cm from the substrate. To avoid fast drilling, the target was mounted on a vacuum compatible, computer-controlled XY-stage and performed a meander-like movement (Fig.1b). The deposition chamber was initially evacuated to a base pressure 10^{-4} Pa. The GaN substrate was tightly mounted on a resistively heated round metallic plate and kept overnight at the desired temperature (at 400 °C) using a stabilized DC current power supply. The temperature was continuously monitored by a Ni–NiCr thermocouple (Philips 2 AB I 15) that was placed inside and at the center of the heated plate just 1mm beneath the substrate. The deposition time was 60 min and the oxygen pressure values were 20 and 30 Pa in a dynamic flow. As it is well known, PLD grown ZnO thin films show n-type conductivity. This was confirmed by Hall effect measurements revealing carrier concentrations ~$7.5x10^{16}$ cm^{-3} and ~$2x10^{17}$ cm^{-3}, for the two thin films. The thickness of both ZnO thin films was about 400 nm, measured by the weighting technique.

2.3 LED electrical contacts

In order to form a diode structure, Pt/Ni/Au alloy was used to form ohmic contact to the p-GaN substrate. The thickness of Pt, Ni, and Au layers were 10 nm, 30 nm, and 80 nm. Non-alloyed Pt/Al metal (with ~50, 70 nm thickness) system was used to form the ohmic contacts on the ZnO films by e-beam evaporation as described in ref. [31].

Nonalloyed ohmic contacts provide smooth interfaces due to limited interface reaction; therefore, they are preferred for the shallow junction devices, operating under low current

density and at low temperature. Alloyed ohmic contacts are the most widely used technique, in which several contact metals are sequentially deposited on ZnO surface, then heated above the eutectic temperature. During annealing, the oxygen atoms can move from the ZnO lattice towards the metal layer, leaving oxygen vacancies near the surface of ZnO [32, 33]. The increase in carrier concentration of the n-type ZnO results in a reduction of the depletion region width. Thus the probability of tunneling is increased and contact resistivity (ρ_c) is dramatically reduced.

Circular LED mesas were fabricated from the heterostructure by masking the surface and chemically etching away the ZnO layer using a dilute acid. Six different masks were used to give mesa areas ranging from 0.04 mm^2 up to 0.40 mm^2 in increments of 0.05-0.07 mm^2 range (Fig.2).

3. Results and Discussion

3.1 Surface and Optical Properties of ZnO Thin Films

Before examining the n-ZnO/p-GaN heterojunction LED properties, we will present ZnO films surface and optical properties for both produced films with sol gel and PLD methods.

As we see from Figs. (3-4), surface maps of the films deposited with PLD have better contours to the samples obtained from sol gel method. The surface morphology of these films show regular arrangement of fine closely packed hexagonal crystallites. The surface roughness of the ZnO films was increased drastically, along with the apparent grain formation with both annealing and increasing oxygen pressure.

The rms (Root mean square) values of the ZnO films grown on GaN/sapphire were found to be 9.76 (20 Pa), 12.00 (30 Pa) and 4.84 (as deposited), 6.46 (annealed at 500 ^oC) nm for PLD and sol gel samples, respectively. A comparison between PLD and sol gel methods indicated that PLD exhibited a higher density with increasing the surface roughness of the films.

Figure (5), shows the Photoluminescence (PL) spectrum of ZnO films fabricated with PLD and sol gel methods under different conditions. Fig. 5 (a), consists of a strong luminescent peak centered at 369 nm is near-band emission (NBE), which corresponds to the exciton emission from near conduction band to valence band. The ZnO near-band-edge emission is attributed to the radiative annihilation of free and bound excitons [34, 35].

Other weak ones located at 377 nm and 383 nm are defect emissions. These deep level luminescences have been reported to originate from defects [36]. Therefore, its weak nature is also an indication of good material quality in our ZnO thin films. The improved crystalline

quality of the ZnO thin films is thought to be a consequence of very small lattice mismatch between ZnO and p-GaN (~1.9%). These results are in a good agreement with the earlier report [37].

Also, Figure 5 (b) has four main emission peaks. Intense peak centered at 387 nm and weak defects emission (violet emissions) bands centered at 401, 407 and 426 nm. Ahn et al. have demonstrated that the violet, green, and orange-red emissions were caused by zinc interstitial (Zn_i), oxygen vacancy (V_O), and oxygen interstitial (O_i) defect levels, respectively [38].

The PL spectra in Figure 5 (a) show that the UV emission of ZnO thin film fabricated on GaN/sapphire substrate with PLD at 30 Pa is higher than one fabricated at 20 Pa and there is a shift towards the blue region. The increase of UV emission and the decrease of the defect emission indicate that the structure obtained at 30 Pa becomes more perfect. The UV peak appears as a redshifts from 369 to 387 nm. The relaxation of interface strain is the main reason because of the formation of ZnO/GaN/sapphire heterostructure. Moreover, no broad band related to deep level emissions was observed in PL spectra of the films. Such emission tails are generally associated with the presence of native defects in ZnO films in the form of oxygen vacancies or point defects. The appearance of such sharp, narrow UV is an indication of the good quality of the ZnO films. On the other side, Figs.5 (c) and (d) show that, sol gel method also concludes films with good optical effects. The as deposited film has UV emission peak centered at 384 nm and no weak defect emission bands were observed. The PL spectra of the annealed ZnO film at 500 °C shows maximum intensity of the peak corresponding to 3.18 eV (390 nm) with relatively low line width ~115 meV. This also confirms the growth of good quality and defect free ZnO films using GaN/ sapphire substrate.

The weak peak at 412 nm is typical for Mg doped GaN films, and is generally attributed to transitions from the conduction band or shallow donors to deep Mg acceptor levels [24]. Other peak (blue emission) located at 455 nm most likely derives from electronic transition from the donor level of Zn interstitial to acceptor energy level of Zn vacancy according to Sun's calculation by full-potential linear muffin-tin orbital method (FP-LMTO) [39-42]. This shows that some Zn_i atoms exist in fabricated ZnO thin films. The emission located at 426 nm may be caused by the electronic transition between the anti-oxygen (O_{Zn}) and the conduction band.

With a general aspect to the whole PL spectra, the intensity of emissions increases throughout the spectra with annealing and increasing of oxygen pressure which is typical due to the increase in nonradiative interface recombination for sol gel and PLD thin films, respectively. Also other important info must be noted that because the ZnO layer has the lower carrier

concentration compared with that of the p-GaN layer, hence, the depletion region of the p–n heterojunction is mostly exist in the n-ZnO region. The holes from p-GaN and electrons from n-ZnO are thereby injected into the ZnO layer to undergo the radiative recombination. Therefore, the radiative recombination occurs mainly at the n-ZnO layer and observing the blue and violet light emission is a usual phenomenon [43].

3.2 LED Applications

To strengthen our results, we must also look Electroluminescence (EL) (with 20 mA of driving current) spectrum of n-ZnO/p-GaN heterojunction LED (Fig. 6). EL spectra at room temperature of n-ZnO/p-GaN heterojunction with ZnO films fabricated at 20 Pa with PLD has three peaks approximately centered at 400 nm (violet emission), 482 nm (blue) and a broad peak at 650 nm (red emission) are observed.

The violet peak is centered at 3.08 eV (400 nm) and it agrees well with the transition energy from Zn_i level to the valence band in ZnO (approximately 3.1 eV). The blue peak (2.58 eV) is attributed to recombination between the Zn_i energy level to the V_{Zn} energy level. There is a difference of 0.26 eV. May be this difference is due to effect of GaN substrate as GaN also emits blue light [44].

At 30 Pa, peaks are observed as green and red emissions located at 495 nm (2.50 eV;) and 625 nm (2.0 eV). Intensity of the peaks shows a slight increase with increasing oxygen pressure. For the samples produced with sol gel method, we have seen a similar tendency of the peaks. In as deposited films, we see two broad main peaks that are in green and red regions. Many intrinsic or extrinsic defects have been reported to produce emission in the visible region, such as intrinsic defects such as oxygen vacancies, antisite oxygen, zinc vacancies or interstitials and surface defects [45-51].

In annealed at 500^{o} C films, three emissions at 350 nm (3.54 eV), 450 nm (2.76 eV) and 580 nm (2.14 eV) were seen. The emission at 350 nm can be attributed to the band edge emissions in p-GaN substrate. This indicates that p-GaN substrates are also of high optical quality. The blue emission at 450 nm can be attributed to transitions between a nitrogen vacancy and a carbon atom in GaN [52, 53]. There is a difference of 0.08 eV between the reported value and the present one. This difference may be due to the effect of the GaN substrate that emits blue light as mentioned above [44, 54].

The third yellow emission at 580 nm (2.14 eV) can be evaluated as lattice defects that such broad yellow band is commonly observed in all GaN layers [54-56]. We think that such

extended defects in the Mg-doped p-type GaN layer are related to the large lattice mismatch between GaN and sapphire (~16 %).

A comparison of EL and PL spectra of the n-type ZnO and p-type GaN layers showed that two EL emission peaks were attributed to a radiative recombination in both n-type ZnO and p-type GaN layers.

Fig.7 shows rectifying characteristics of a n-ZnO/p-GaN heterojunction with the forward turn-on voltage of 11 V, 12.5 V for 30 Pa and 20 Pa also 14 V for both as deposited and annealed films, respectively. The large turn-on voltage should be attributed to the large p contact resistance. The linear I–V characteristics on n-ZnO contacts and on p-GaN contacts also indicate that the contacts have good ohmic properties. This shows that we indeed achieved a rectifying I–V curve.

4. Conclusions

On the basis of these results, we propose a significant detail for making a LED involving different fabrications as shown in the inset of Fig. 2. We tried to show that how different ZnO growth methods affect the whole device performance. This introduction contains Pulsed Laser Deposition (PLD) system as representative of physical process and Sol gel method as representative of chemical process. Only oxygen pressure effect on LED characterization has not been reported yet as a single parameter and it was concluded that oxygen pressure made a strong effect on ZnO films quality; for sol gel method, annealing contributed a great improvement for the ZnO films. Room-temperature PL results have narrow, sharp and high quality peaks that also means high quality ZnO thin films in the sense of optical characteristics. These emissions were observed at 369 nm and 387 nm for PLD films and at 384 nm and 390 nm for Sol gel films evaluated as the near-band emission (NBE), which corresponds to the exciton emission from near conduction band to valence band. Other weak peaks were attributed to the defect emissions.

Electroluminescence (EL) peaks were observed at expected wavelengths and in reported regions. Annealing made a significant improvement on peaks with narrower and higher intensity. On PLD films, increasing oxygen pressure made also narrower, sharper and higher peaks of the emissions. A clear rectifying behavior of the ZnO/GaN p-n heterojunction was demonstrated by the I–V curve. The I–V curve of the ZnO LED showed a good rectification characteristic with an unnoticeable low leak current and good ohmic properties of the diode contacts.

The high UV emission of ZnO/GaN/sapphire films and the less defect emission with Zn_i and V_o reveal that the film possesses high quality by introducing a GaN layer with a proper mobility and carrier concentration on sapphire. In conclusion, it is favorable to fabricate high emission efficiency ZnO thin film on GaN/sapphire substrate rather than other candidates such as Si, AlGaN, MgZnO, $CuAlO_2$ or polymer structures. This systematic study provides an opportunity to see the optimized conditions and for constructing the ideal ZnO/GaN heterostructure and deep UV emission LED devices.

Acknowledgements

The authors are honored due to their technical support of Laser-based Techniques and Applications (LATA) Theor. & Phys./Chem. Institute (NREL), GREECE and also financial support of Gaziosmanpaşa University, TURKIYE Scientific Research Council with the Grand Contract No: 2010/16.

References

[1] D. C. Reynolds, D. C. Look and B. Jogai, Solid State Commun. 99 (1996) 873.

[2] D. M. Bagnall, Y. F. Chen, Z. Zhu, T. Yao, S. Koyama, M. Y. Shen and T. Goto, Appl. Phys. Lett. 70 (1997) 2230.

[3] R. D. Vispute, V. Talyansky, S. Choopun, R. P. Sharma, T. Venkatesan, M. He, X. Tang, J. B. Halpern, M. G. Spencer, Y. X. Li, L. G. Salamanca-Riba, A. A. Iliadis and K. A. Jones, Appl. Phys. Lett. 73 (1998)348.

[4] E.-C. Lee, Y.-S. Kim, Y.-G. Jin and K. J. Chang, J. Korean Phys. Soc. 39 (2001) S23.

[5] K. J. Yee, I. H. Lee, K. G. Lee, E. Oh and D. S. Kim, J. Korean Phys. Soc. 42 (2003) S157.

[6] D. C. Look, Mater. Sci. Eng. B 80 (2001) 383.

[7] J.M. Bian, X.M. Li, X.D. Gao, W.D. Yu, L.D. Chen, Appl. Phys. Lett. 84 (2004) 541.

[8] D.C. Look, D.C. Reynolds, C.W. Litton, R.L. Jones, D.B. Eason, G. Cantwell, Appl. Phys. Lett. 81 (2002) 1830.

[9] T. Ive, T. Ben-Yaacov, CGV. De Walle, UK. Mishra, SP. Denbaars, JS. Speck, J Cryst Growth 310 (2008) 3407.

[10] JH. Kim, EM. Kim, D. Andeen, D. Thomson, SP. Denbaars, FF. Lange, Adv Funct Mater 17 (2007) 463.

[11] JY. Lee, HS. Kim, HK. Cho, YY. Kim, BH. Kong, HS. Lee, Jpn J Appl Phys 47(2008) 6251.

[12] M. Dutta, D. Basak, Appl. Phys. Lett. 92 (2008) 212112.

[13] M.P. Bhole, D.S. Patil, Optoelectron. Adv. Mater.-Rapid Commun. 1 (2007) 672.

[14] Y.J. Lin, P.H.Wu, C.L. Tsai, C.J Liu, Z.R. Lin, H.C Chang, C.T Lee, J. Appl. Phys. 103 (2008)113709.

[15] Y.J. Lin, P.H.Wu, C.L. Tsai, C.J Liu, C.T Lee, H.C. Chang, Z.R. Lin, K.Y Jeng, J. Phys. D Appl. Phys. 41 (2008)125103.

[16] M. Stamataki, I. Fasaki, G. Tsonos, D. Tsamakis, M. Kompitsas, Thin Solid Films 518 (2009)1326-1331.

[17] M.G. Tsoutsouva, C.N. Panagopoulos, D. Papadimitriou, I. Fasaki, M. Kompitsas, Mater. Sci. Eng. B 176 2011)480-483

[18] J.H. Kim, E.M. Kim, D. Andeen, D. Thomson, S.P. Denbaars, F.F. Lange, Adv. Funct. Mater. 17 (2007) 463.

[19] D.J. Rogers, F.H. Teherani, A. Yasan, K. Minder, P. Kung, M. Razeghi, Appl. Phys. Lett. 88 (2006) 141,918.

[20] T. P. Yang, H. C. Zhu, J. M. Bian, J. C. Sun, X. Dong, B. L. Zhang, H. W. Liang, X. P. Li, Y. G. Cui, and G. T. Du, Mater. Res. Bull., 43(12) (2008) 3614–3620.

[21] J. Young Lee, J. Hoon Lee , H. Seung Kim, C.-Hyun Lee, H.-Soo Ahn, H. Koun Cho, Y. Yi Kim, B. Hyun Kong , H. Seong Lee, Thin Solid Films 517 (2009) 5157–5160.

[22] D. K. Hwang, S. H. Kang, J. H. Lim, E. J. Yang, J. Y. Oh, J. H. Yang, and S. J. Park, Appl. Phys. Lett. 86 (22)(2005) 222.

[23] L. J. Mandalapu, Z. Yang, S. Chu, and J. L. Liua, Appl. Phys. Lett., 92(12) (2008) 122.

[24] W. I. Park and G. C. Yi, Adv. Mater.16 (1) (2004) 87–90.

[25] H. Sun, Q. F. Zhang, and J. L. Wu, Nanotechnology, vol. 17(9) (2006) 2271–2274.

[26] B. Ling, X. W. Sun, J. L. Zhao, S. T. Tan, Z. L. Dong, Y. Yang, H. Y. Yu, and K. C. Qi, Phys. E, vol. 41.(4) (2009) 635–639.

[27] A. Nadarajah, R. C. Word, J. Meiss, and R. Konenkamp, Nano Lett., 8 (2008) 534–537.

[28] D. Rogers, F.H. Teherani, P. Kung, K. Minder, M. Razeghi, Superlattice Microst. 42 (2007) 322–326.

[29] A. Yasan, R. McClintock, S.R. Darvish, Z. Lin, K. Mi, P. Kung, M. Razeghi, Appl. Phys. Lett. 80 (2002) 2108.

[30] Z. Lamia, Mat Sci Eng B 174 (2010) 18–30.

[31] H. K. Kim, K. Kim, S. Park, T. Seong, and I. Adesida, J. Appl. Phys. 94 (2003) 4225.

[32] H.K. Kim, T.Y. Seong, K.K. Kim, S.-J. Park, Y. S. Yoon, and I. Adesida, Jpn. J. Appl. Phys. 43, (2004) 976.

[33] L.J. Brillson, Y. Lu, J. Appl. Phys. 109 (2011)121301.

[34] P. Zu, Z. K. Tang, G. K. L. Wong, M. Kawasaki, A. Ohtomo, H. Koinuma, and Y. Segawa, Solid State Commun. 103(1997) 459-463.

[35] X. Wang, J. Cole, A. M. Dabiran, H. O Jacobs, NSTI-Nanotech 2007, 4(2007) 526-529.

[36] F.K. Shan, G. Lee, X.W.J. Lee, G.H. Lee, I.S. Kim, B.C. Shin, Appl. Phys. Lett. 86 (2005) 221910.

[37] J.H. Kim, E.M. Kim, D. Andeen, D. Thomson, S.P. DenBaars, F.F. Lange, Adv. Funct. Mater. 17 (2007) 463.

[38] C.H. Ahn, Y.Y. Kim, D.C. Kim, S.K. Mohanta, H.K. Cho, J. Appl. Phys. 105 (2009) 013502.

[39] XQ Wei, BY Man, CS Xue, CS Chen, M. Liu, Jpn J Appl Phys, 45(11) (2006) 8586.

[40] XQ Wei, BY Man, AH Liu, Yang C, CS Xue, HZ Zhuang, Physica B, 388 (1–2) (2007)145.

[41] B. Lin, Z. Fu, Y. Jia, Appl Phys Lett, 79(7)(2001) 943.

[42] X. Wei, R. Zhao, M. Shao, X. Xu, J. Huang, Nanoscale Res Lett, 8 (2013)112.

[43] J. Y. Lee, J. H. Lee, H. S. Kim, C.H. Lee, H.S. Ahn, H. K. Cho,Y.Y. Kim, B. H. Kong, H. S. Lee, Thin Solid Films 517 (2009) 5157–5160.

[44] N.H. Alvi , M. Willander , O. Nur, Superlattice Microst 47 (2010) 754-761.

[45] D.M. Bagnall, Y.F. Chen, Z. Zhu, T. Yao, S. Koyama, M.Y. Shen, T. Goto, Appl. Phys. Lett. 70 (1997) 2230.

[46] O. Lupan, T. Pauporte, B. Viana, I.M. Tiginyanu, V.V. Ursaki, R. Cortes, ACS Appl. Mater. Interfaces 2 (2010) 2083.

[47] T.S. Herng, S.P. Lau, S.F. Yu, S.H. Tsang, K.S. Teng, J.S. Chen, J. Appl. Phys. 104 (2008) 103104.

[48] C.X. Xu, X.W. Sun, X.H. Zhang, L. Ke, S.J. Chua, Nanotechnology 15 (2004) 856.

[49] S. Eustis, D.C. Meier, M.R. Beversluis, B. Nikoobakht, ACS Nano 2 (2) (2008) 368.

[50] U. Ozgur, Ya.I. Alivov, C. Liu, A. Teke, M.A. Reshchikov, S. Dogan, V. Avrutin, S.J. Cho, H.A. Morkoc, J. Appl. Phys. 98 (2005) 041301.

[51] X.B. Wang, C. Song, K.W. Geng, F. Zeng, F. Pan, Appl. Surf. Sci. 253 (2007) 6905.

[52] P. Klason, T.M. Borseth, Q.X. Zhao, B.G. Svensson,A.Y. Kuznetsov, P.J. Bergman, M. Willander, Solid State Commun. 145 (2008) 321.

[53] C.H. Ahn, Y. Yi Kim, D. Chan Kim, S. K. Mohanta, H. K. Cho, J. Appl. Phys. 105 (2009) 013502.

[54] I.E. Titkov, A.S. Zubrilov, L.A. Delimova, D.V. Mashovets, I.A. Liniichuk, I.V. Grekhov, Semiconductors 41 (2007) 564–569.

[55] S. Nakamura, S.F. Chichibu (Eds.), Introduction to Nitride Semiconductor Blue Lasers and Light Emitting Diodes, CRC Boca Raton, New York, 2000.

[56] S.H. Hwang, T.H Chung, B.T Lee, Mat. Sci. Eng. B 157 (2009) 32–35.

LIST OF FIGURES CAPTIONS

Fig. 1 a) Spin coating system

b) The side view of PLD system used for ZnO thin films production.

Fig. 2 A schematic diagram and image of the ring mesas of n-ZnO/p-GaN LED.

Fig. 3 AFM images of ZnO thin films produced with PLD a) 20 Pa b) 30 Pa.

Fig. 4 AFM images of ZnO thin films produced with Sol Gel a) as deposited b) annealed at 500 °C.

Fig. 5 Photoluminescence (PL) spectra of ZnO thin films produced on p-GaN:Mg /Sapphire (0 0 0 1) heterostructure a) PLD (20 Pa) b PLD (30 Pa) c) Sol gel (as deposited) d)Sol gel annealed at 500 ^{o}C

Fig. 6 Electroluminescence spectra (EL) of n-ZnO/p-GaN:Mg /Sapphire (0 0 0 1) heterostructure LED a) PLD (20 Pa) b PLD (30 Pa) c) Sol gel (as deposited) d)Sol gel annealed at 500 ^{o}C .

Fig. 7 I-V curve of n-ZnO/p-GaN heterostructures at room temperature.

a)

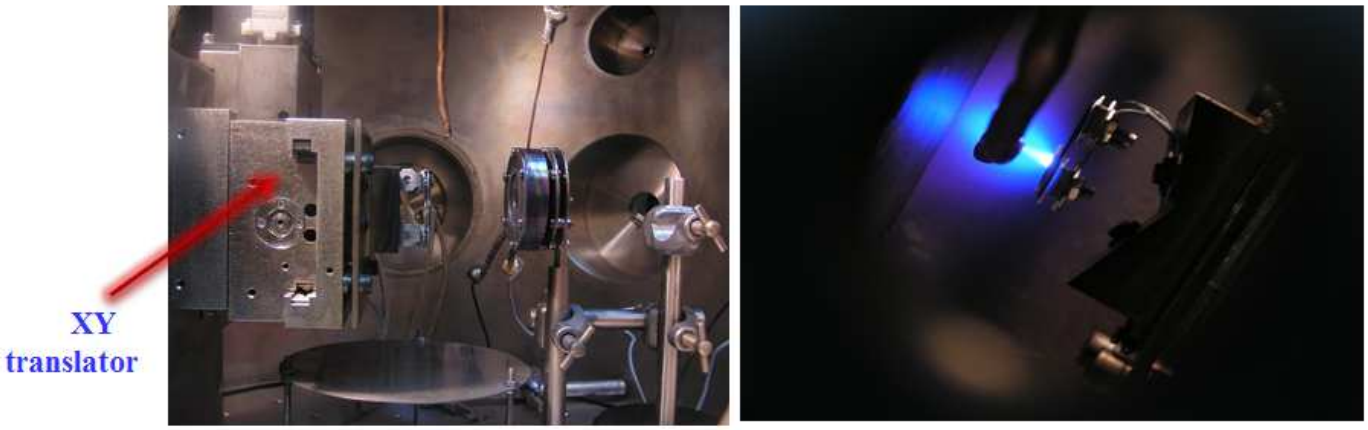

b)

Fig. 1 a) Spin coating system
b) The side view of PLD system used for ZnO thin films production

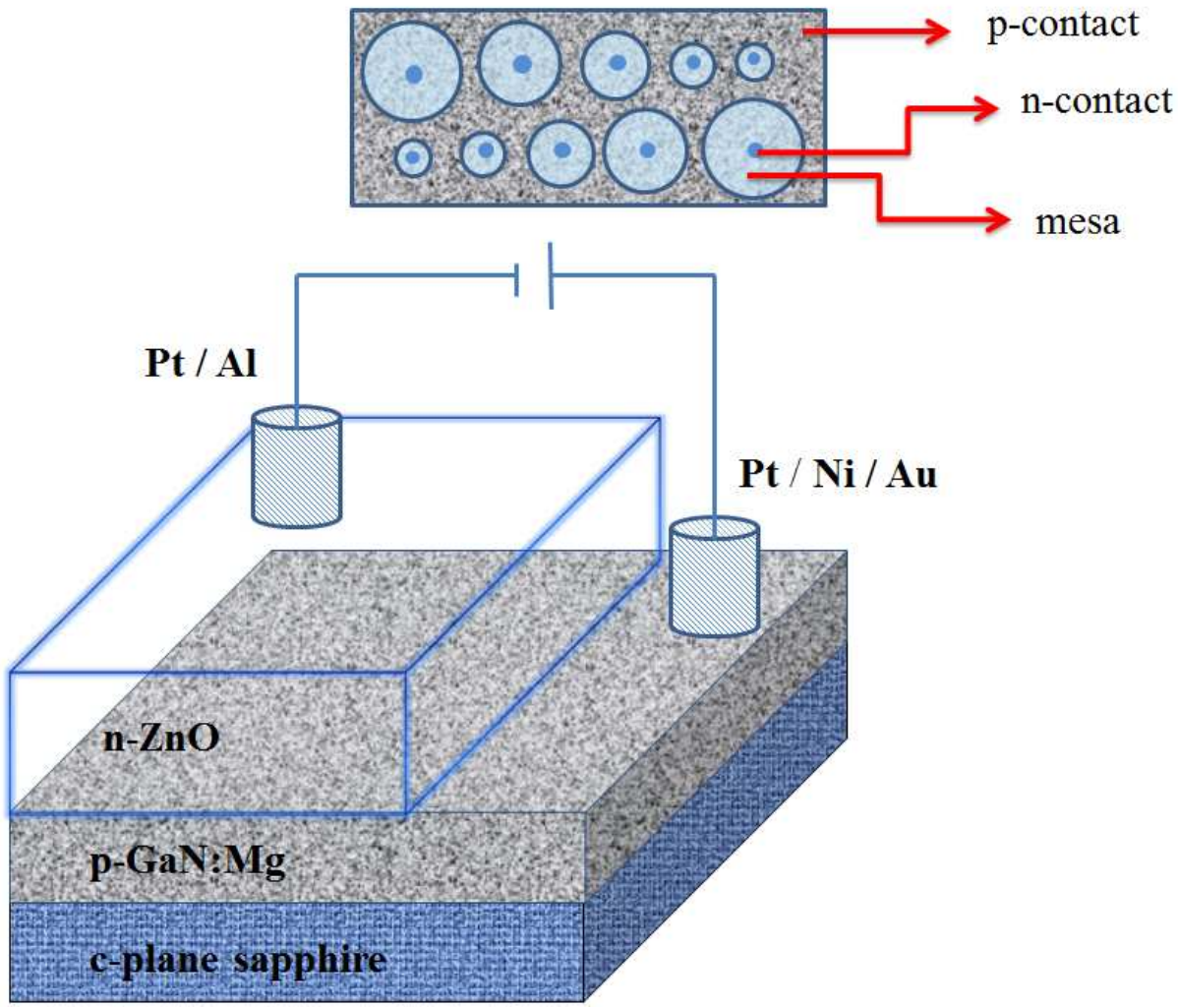

Fig. 2 A schematic diagram and image of the ring mesas of n-ZnO/p-GaN LED.

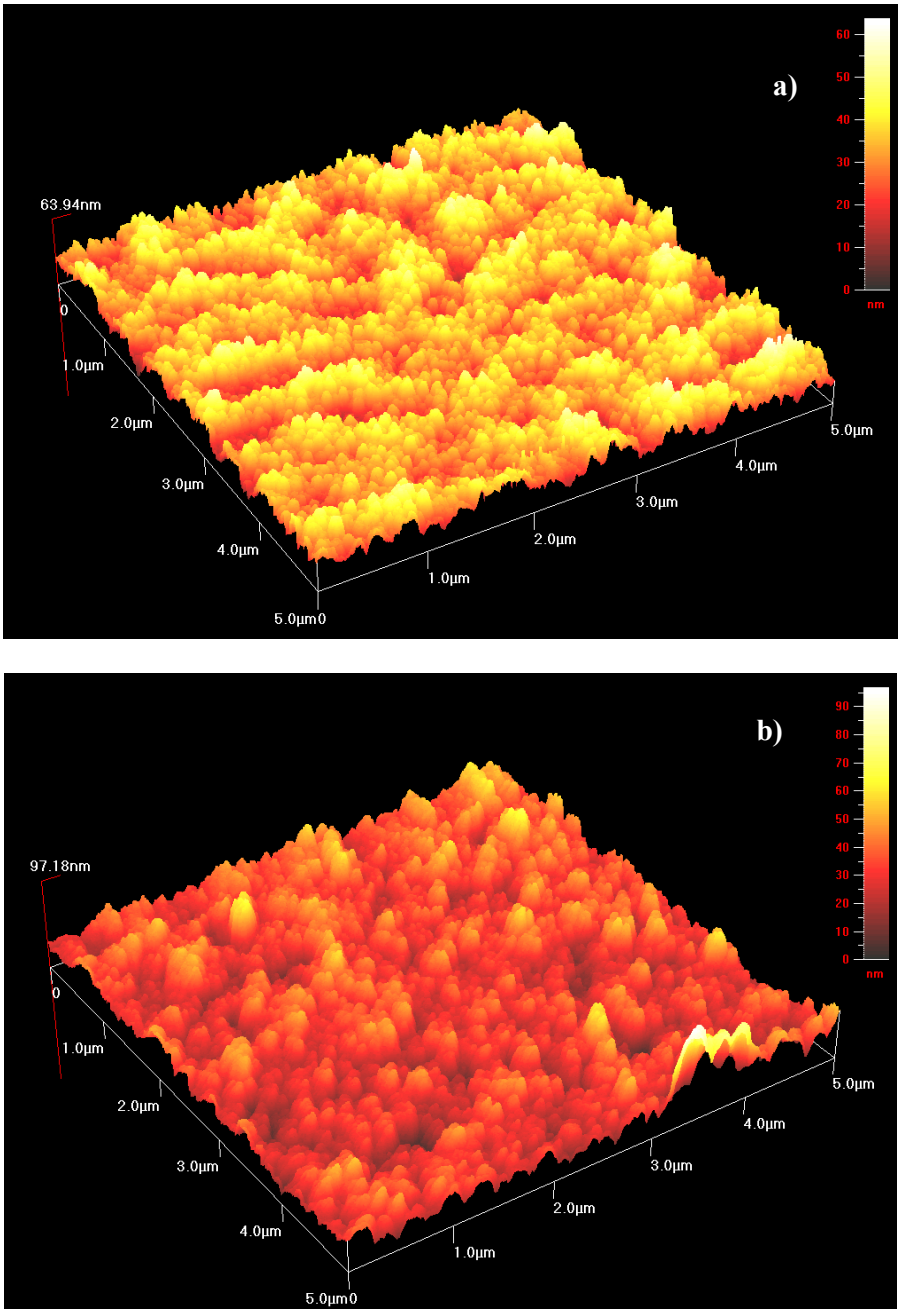

Fig. 3 AFM images of ZnO thin films produced with PLD a) 20 Pa b) 30 Pa.

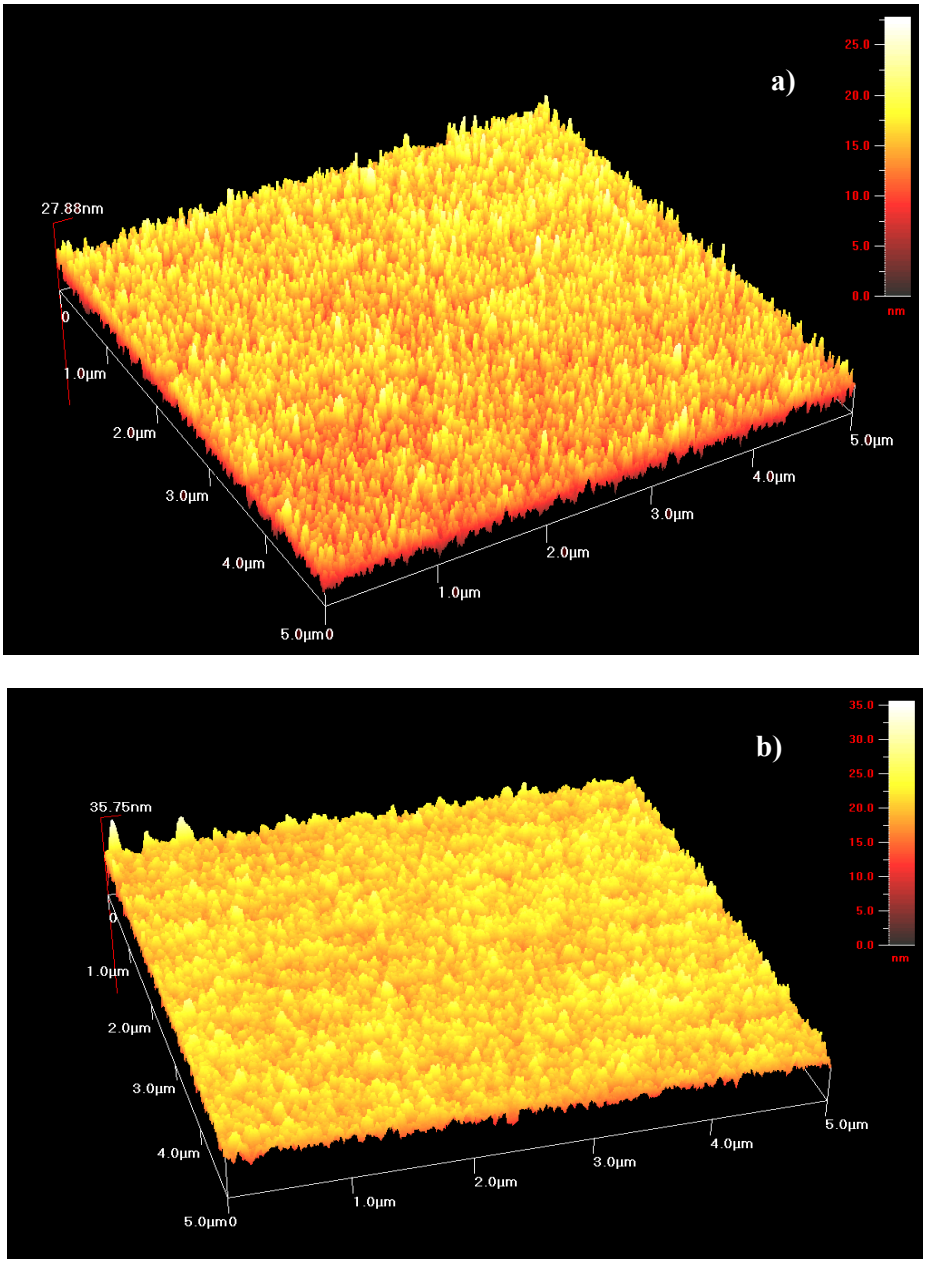

Fig. 4 AFM images of ZnO thin films produced with Sol Gel a) as deposited b) annealed at 500 °C.

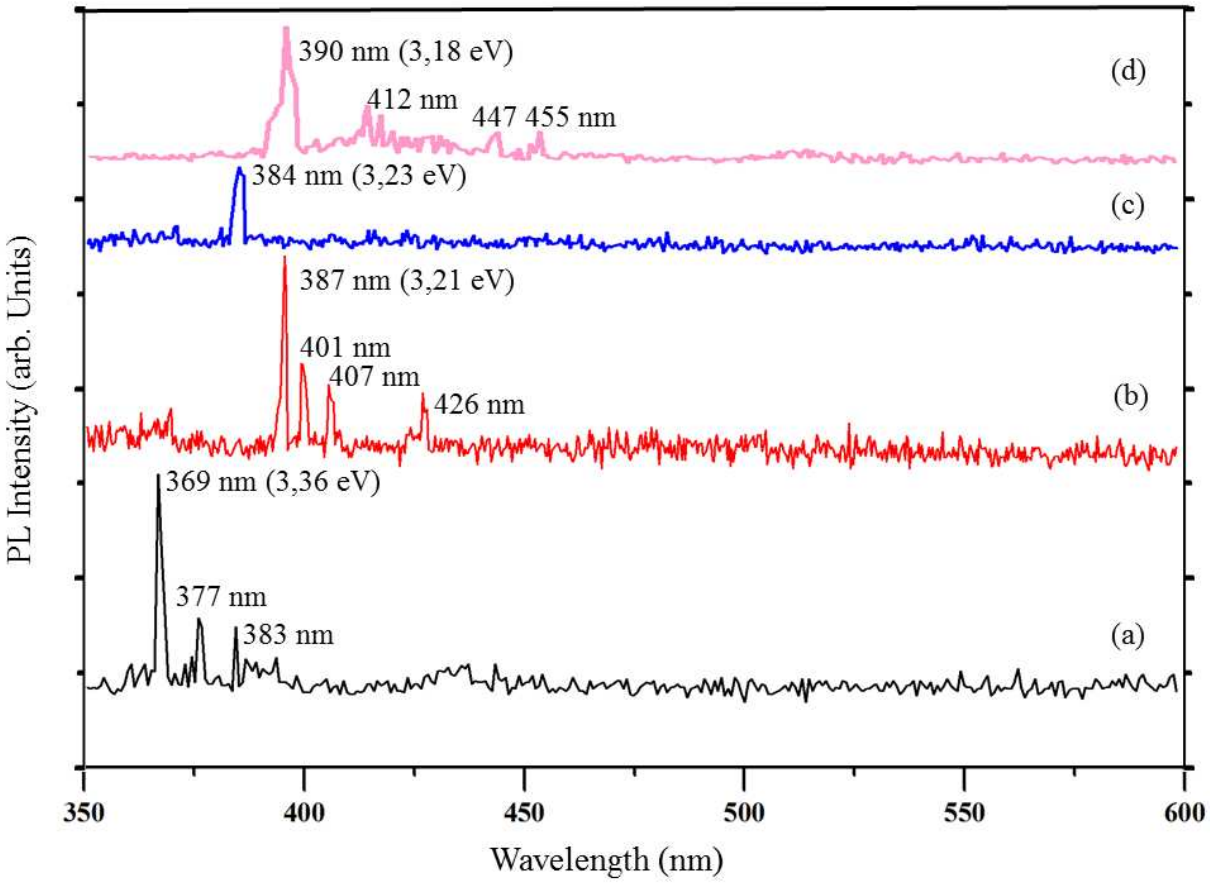

Fig. 5 PL spectra of ZnO thin films produced on p-GaN:Mg /Sapphire (0 0 0 1) heterostructure a) PLD (20 Pa) b PLD (30 Pa) c) Sol gel (as deposited) d)Sol gel (annealed at 500 ^{o}C).

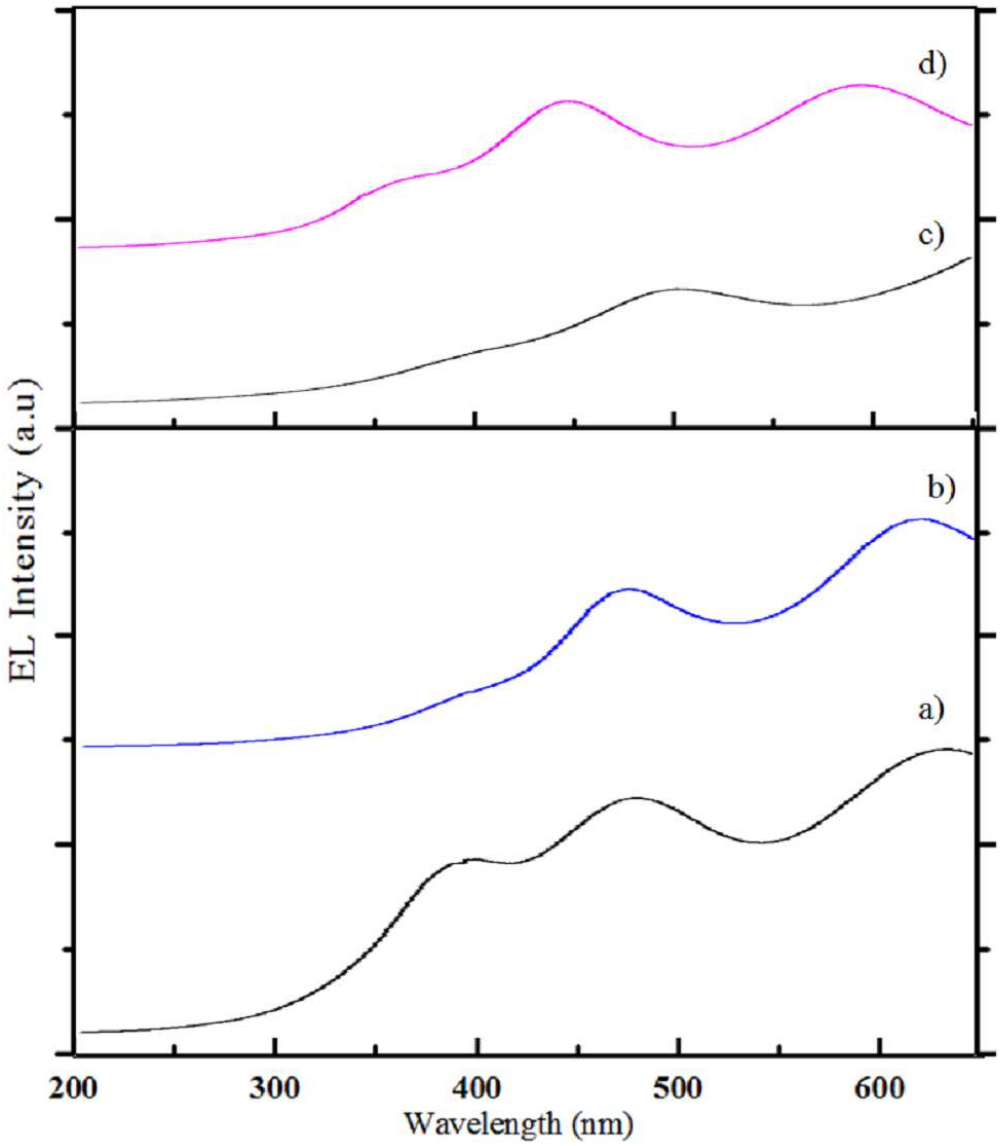

Fig.6 Electroluminescence spectra of n-ZnO/p-GaN:Mg /Sapphire (0 0 0 1) heterostructure LED a) PLD (20 Pa) b PLD (30 Pa) c) Sol gel (as deposited) d)Sol gel (annealed at 500 ^{o}C).

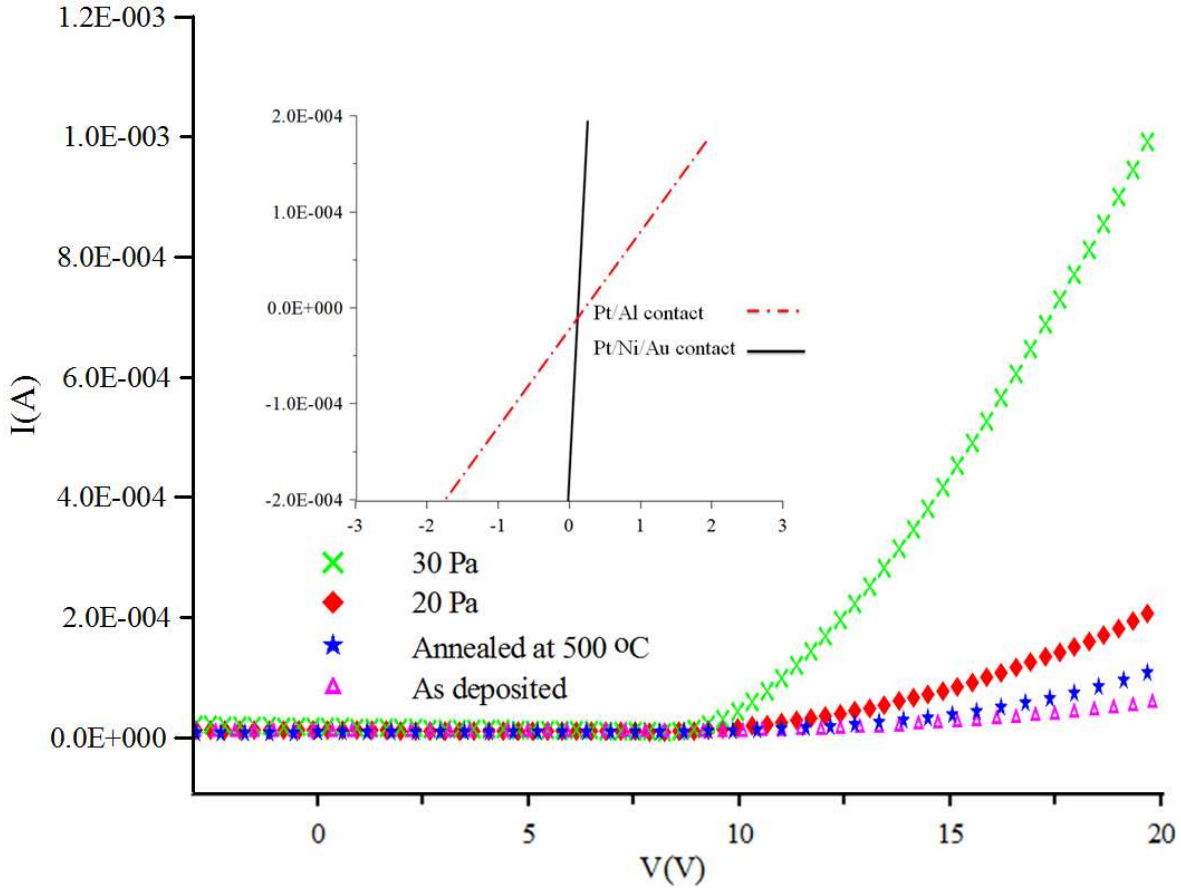

Fig. 7 I-V curve of n-ZnO/p-GaN heterostructures at room temperature.